A Coherent Photoacoustic Approach to Excited-State–Excited-State Absorption Spectroscopy: Application to the Investigation of a Near-Resonant Contribution to Ultrasonic Diffraction

R. J. Dwayne Miller,† Marc Pierre,‡ Todd S. Rose, and M. D. Fayer*

Department of Chemistry, Stanford University, Stanford, California 94305 *(Received: October 3, 1983)*

The previously reported coherent photoacoustic method for measuring weak absorptions is extended to excited-state–excited-state spectroscopy for which conventional acoustic and thermal lensing techniques are greatly reduced in sensitivity. The method involves a picosecond pulse sequence with four pulses. The first pulse populates the excited state. Then, a pair of time coincident pulses cross in the sample, making an optical interference pattern and generating an acoustic diffraction grating. The amplitude of the acoustic grating is proportional to the excited-state–excited-state absorption cross section. The amplitude is measured by the Bragg diffraction of the fourth pulse from the acoustic grating. This method can be readily applied to liquids, glasses, or crystals. Excited-state absorption at 532 nm by the S_1 state of pentacene in *p*-terphenyl host crystals is examined at room temperature and 1.4 K. The results are used in addressing the mechanism for acoustic diffraction of a probe beam nearly resonant with a strong and narrow ground-state transition, e.g., pentacene in *p*-terphenyl at 1.4 K. It is demonstrated that there is a density wave induced spectral shift contribution to the acoustic grating which results in greatly increased diffraction efficiency near resonance.

Introduction

Recently, the development of optoacoustic spectroscopy[1] has made possible the measurement of exceedingly weak absorption spectra for transitions which originate in the system's ground state. However, the tremendous gain in sensitivity afforded by acoustic or thermal lensing[2] spectroscopy over conventional techniques cannot be realized in the study of transitions from an excited state to higher lying excited states.

In the past several years a technique has been developed for the optical holographic excitation and optical detection of tunable ultrasonic waves in liquids, glasses, liquid crystals, and mixed and pure crystals.[3,4] The method involves crossed picosecond laser pulses which set up an optical interference pattern in the sample and thereby excite counterpropagating ultrasonic waves whose wavelength and orientation match those of the interference pattern. The ultrasonic waves are detected by Bragg diffraction of a third laser pulse from what is basically an acoustic hologram (see Figure 1). In addition to a variety of applications in the study of acoustic phonon phenomena, it has also been demonstrated that coherent photoacoustic spectroscopy can be used to measure very weak absorption spectra, e.g., a spectrum of the fifth vibrational overtone of the benzene C–H stretching mode.[5]

Coherent photoacoustic spectroscopy shares a common feature with optoacoustic spectroscopy in that it detects the absorption of light by nonradiative relaxation processes which produce phonons. However, with the present technique, the phonons are generated coherently, which provides the potential for the increased sensitivity that usually accompanies coherent measurements.

We have now extended this spectroscopic approach to the measurement of excited-state–excited-state absorption spectra. This is an important development since conventional acoustic or thermal lensing spectroscopy cannot be readily applied to excited-state–excited-state absorptions. Basically, the current method is to excite S_1 with one light source, then pass a second light source through the sample to look for absorptions not present when S_1 is unpopulated. This works for strong absorptions. The problem with acoustic spectroscopy in this application is that the energy used to excite S_1 will itself produce a large acoustic signal, obscuring the acoustic signal produced by weak $S_1 \rightarrow S_n$ transitions. Recently there have been experiments in the time domain using picosecond pulses which separate the acoustic signal arising from ground-state transitions from the acoustic signal produced by excited-state transitions using fast electronics.[6] However, much of the sensitivity of ground-state acoustic spectroscopy is lost. Sensitive electronic methods are being developed for the acoustic measurement of excited-state spectra.[7] This approach has been shown to be 40 times more sensitive than conventional optical pump probe experiments. The acoustic approach described here has the potential for bringing the great sensitivity of ground-state acoustic spectroscopy to the measurement of excited-state spectra.

The coherent photoacoustic approach avoids the problem of an acoustic signal arising from the S_0 to S_1 pumping by using the inherent advantages of a nonlinear holographic method. The experiment is a four-pulse sequence (see Figure 1). The first pulse (a single beam) excites the sample from S_0 to S_1. Then a pair of tunable wavelength crossed pulses set up an optical interference pattern in the sample. If there is excited-state absorption, a grating pattern of high lying excited states will be produced. These S_n excitations will rapidly ($\lesssim$10 ps) relax to S_1, producing local heating. The heat, having a periodic spatial pattern which mimics the optical interference pattern, launches the ultrasonic waves.[4] The amplitude of the wave is detected by Bragg diffraction of a fourth probe pulse off of the induced holographic acoustic grating.[8] This amplitude is proportional to the S_1 to S_n absorption coefficient. The elegance of the approach is that the single pulse (no interference pattern) which takes the system from S_0 to S_1 also produces heat but does not form a diffraction grating. Consequently, the heat from exciting S_1 does not contribute to the signal. Thus, the four-pulse sequence provides a method for the extension of acoustic spectroscopy to the detection of very weak excited-state–excited-state absorptions. The technique should make it possible to measure absolute excited-state absorptivities, if the ground-state absorptivity is known. The parameters of the medium, i.e., heat capacity, thermal expansion coefficient, and op-

†Permanent address: Department of Chemistry, University of Rochester, River Station, Rochester, NY 14627.
‡Permanent address: Laboratoire de Spectrométrie Physique, Université I, 38041 Grenoble, France.

(1) C. K. N. Patel, A. C. Tam, and R. J. Kerl, *J. Chem. Phys.*, **71**, 1470 (1979).
(2) M. E. Long, R. L. Swafford, and A. C. Albrecht, *Science*, **191**, 183 (1973).
(3) K. A. Nelson, R. J. D. Miller, D. R. Lutz, and M. D. Fayer, *J. Appl. Phys.*, **53**, 1144 (1982).
(4) K. A. Nelson and M. D. Fayer, *J. Chem. Phys.*, **72**, 5202 (1980).
(5) R. J. D. Miller, R. Casalegno, K. A. Nelson, and M. D. Fayer, *Chem. Phys.*, **72**, 371 (1982).
(6) Mark Bernstein, Lewis J. Rothberg, and K. S. Peters, *Chem. Phys. Lett.*, **91**, 315 (1982); Lewis J. Rothberg, Mark Bernstein, and K. S. Peters, *J. Chem. Phys.*, **79**, 2569 (1983); Jena-Marc Heritier and A. E. Siegman, *IEEE J. Quantum Electron.*, **19**, 1551 (1983).
(7) G. G. Yee and D. S. Kliger, *J. Phys. Chem.*, **87**, 1887 (1983).
(8) K. A. Nelson, R. Casalegno, R. J. D. Miller, and M. D. Fayer, *J. Chem. Phys.*, **77**, 1144 (1982).

0022-3654/84/2088-3021$01.50/0

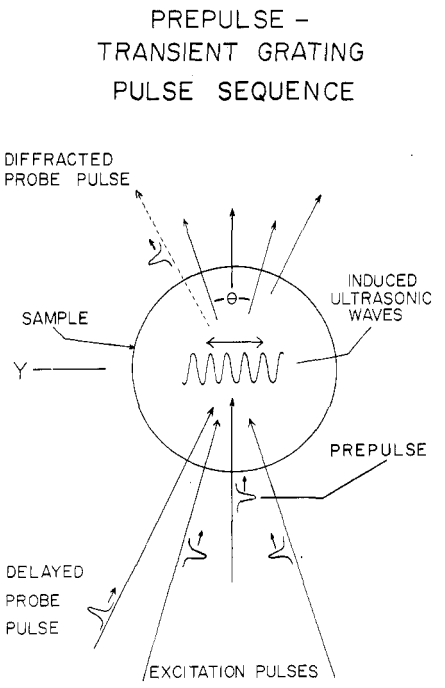

Figure 1. The pulse sequence used for excited-state coherent photoacoustic spectroscopy. The prepulse populates the excited state. The crossed excitation pulses of wavelength λ then produce an acoustic holographic grating which has an amplitude proportional to the excited-state–excited-state absorption cross section at λ. The grating amplitude is measured by Bragg diffraction of the probe pulse.

toelastic constant, need not be known, since they will divide out if the excited-state acoustic effect is compared to the analogous ground-state experiment.[5]

In the experiments presented below, coherent photoacoustic spectroscopy is used to investigated excited-state absorption at 532 nm (doubled Nd:YAG) by pentacene guest molecules in a *p*-terphenyl host crystal at room temperature and 1.4 K. The results demonstrate that there is extensive excited-state absorption at room temperature, but due to reduced line widths at low temperature, there is no 532-nm excited-state absorption at 1.4 K. These results are used to address the question of the mechanism responsible for diffraction by the acoustic grating at 1.4 K. In all experiments to date, diffraction of a probe beam is due to changes in the real part of the bulk index of refraction because of number density changes produced by the acoustic wave. However, if the probe beam wavelength is near resonance with a strong, narrow absorption line, as in the 1.4 K experiments, there is an additional and potentially greater contribution to the diffraction from density-dependent shifting of the spectral position of the resonant transition.[8] The acoustic wave (density wave) generates spatially periodic, time-dependent, spectral shifts which change the real and imaginary contributions of the resonant transition to the sample's index of refraction. If the transition is strong and narrow, the spectral shift contribution to the acoustic diffraction can far exceed the bulk density variation contribution. The experiments on pentacene in *p*-terphenyl at 1.4 K suggest that this is the case for this system.

Mathematical Formulation

In a coherent photoacoustic experiment, two time coincident picosecond pulses are crossed inside the sample to form an optical interference pattern. The resulting sinusoidal variation in light intensity generates counterpropagating ultrasonic waves by inducing material displacements of the same geometry. The material displacements arise either from direct coupling of the light's $\vec{E}$ field to material fields via electrostriction[9] or from absorptive heating with subsequent thermal expansion.[4] In most situations the electrostrictively generated ultrasonic wave is negligible.[3] It has been treated previously in the application of coherent photoacoustic spectroscopy to ground-state systems.[5] The same treatment applies here, and it will not be considered further.

In optically absorbing samples, heat deposited into the lattice at the interference maxima on a time scale short relative to the acoustic period causes impulsive thermal expansion, which drives material, in phase, away from the interference peaks toward the nulls. This launches ultrasonic waves in both directions along the grating. The acoustic wavelength is the same as the distance between interference maxima, i.e.

$$\Lambda = \frac{\lambda}{2 \sin \theta/2} \tag{1}$$

where λ is the wavelength in air of the two excitation pulses, θ is the angle between the pulses in air, and Λ is the acoustic wavelength.

The thermally induced strain, S, is given by[4]

$$S = A \cos (ky)[1 - \cos (\omega t)] \tag{2}$$

where $k = 2\pi/\Lambda$ is the acoustic wave vector, y is the propagation direction, and ω is the acoustic frequency ($\omega/k = v_p$ the speed of sound), and A is the acoustic amplitude. For an isotropic medium or acoustic propagation along a pure mode direction in anisotropic solids, the acoustic amplitude is given by

$$A = (c_{11} + 2c_{12})\alpha \Delta T_m \frac{k^2}{2\omega^2 \rho_0} \tag{3}$$

where c_{11} and c_{12} are the materials elastic constants,[10,11] α is the linear coefficient of thermal expansion,[11] and ρ_0 is the normal density. ΔT_m is the temperature jump at the interference maxima

$$\Delta T_m = \frac{q\beta I_m}{\rho_0 C_v} \tag{4}$$

where q (erg photon^{-1}) is the fraction of the absorbed photon's energy immediately deposited into the lattice as heat, β (cm^{-1}) is the absorptivity per unit length, I_m (photons cm^{-2}) is the integrated light intensity at the interference peaks, and C_v (erg k^{-1} g^{-1}) is the constant volume heat capacity. The important feature of eq 3 and 4 is that the acoustic amplitude is proportional to the absorptivity of the sample at the wavelength λ.

The ultrasonic strain wave creates spatially periodic variations in the density of the sample. These density variations cause spatial variations in the index of refraction and the formation of a diffraction grating. The amplitude of the acoustic response can be determined by Bragg diffraction of a probe pulse off the acoustic phase grating. The efficiency of light diffraction, in the low diffraction limit, is given by[8,12-14]

$$\eta = \left(\frac{\pi l}{\lambda_p \cos \phi}\right)^2 \Delta n^2 \tag{5}$$

where η is the diffraction efficiency, λ_p is the probe wavelength in air, l is the grating thickness, ϕ is the appropriate Bragg angle, and Δn is the peak–null variation in the index of refraction. For the ultrasonic strain described by eq 2, the peak–null difference in n, Δn_s, is given by[5,8]

$$\Delta n_s = -\left(\frac{\rho \partial n}{\partial \rho}\right)\Delta S = -2\left(\frac{\rho \partial n}{\partial \rho}\right)[A(1 - \cos (\omega t))] \tag{6}$$

where ΔS is the peak–null difference in strain from eq 2, ρ is the density, and $(\rho \partial n/\partial \rho)$ is the optoelastic constant. If the optoelastic constant of the bulk material is known, the acoustic amplitude

(9) K. A. Nelson, D. R. Lutz, M. D. Fayer, and L. Madison, *Phys. Rev. B*, **24**, 3261 (1981).

(10) B. A. Auld, "Acoustic Fields and Waves in Solids", Vol. I, Wiley, New York, 1973.

(11) "American Institute of Physics Handbook", 3rd ed., D. E. Gray, Ed., McGraw-Hill, New York, 1972.

(12) H. Kogelnik, *Bell System Tech. J.*, **48**, 2909 (1969).

(13) A. B. Bathia and W. J. Noble, *Proc. R. Soc. London, Ser. A*, **220**, 356 (1953).

(14) W. R. Klein and B. D. Cook, *IEEE Trans.*, **SU-14**, 123 (1967).

can be determined by measuring the diffraction efficiency. The sample's absorption cross section can then be determined from the quantitative description of the acoustic response given by eq 3 and 4. For experimental reasons, it is generally easier to obtain the absolute absorption cross section by comparison of the unknown to an absorption standard,[5] which in this case can be the ground-state transition of the same sample. With a standard, it is unnecessary to know the sample's optoelastic constant and other parameters. In all cases the relative absorption cross section is obtained directly from the experiment.

The use of coherent photoacoustic spectroscopy to study excited-state transitions requires that the excited state under investigation be populated by an excitation pulse prior to the grating excitation pulse sequence (see Figure 1). The acoustic response to this excitation prepulse is spatially slowly varying, and there is no sinusoidal material displacements which give rise to an acoustic wave. Thus, there is no contribution from the ground-state absorption of the prepulse to the detected acoustic signal.

There are three distinct wavelength ranges associated with the application of coherent photoacoustic spectroscopy to excited-state measurements. They are (1) wavelengths to the red of the $S_0 \rightarrow S_1$ transition energy, (2) the wavelength of the $S_0 \rightarrow S_1$ origin and wavelengths somewhat to the blue, and (3) wavelengths well to the blue of the $S_0 \rightarrow S_1$ origin. In range (1) the optical interference pattern excites only $S_1 \rightarrow S_n$ transitions. Then following rapid radiationless relaxation, the only grating is the acoustic grating. A spectrum is taken by exciting the sample to S_1 with the prepulse, the recording the amplitude of the oscillations in the diffracted signal as a function of the wavelength of the crossed excitation pulses.

In range (2), the excitation pulses will not only be absorbed by $S_1 \rightarrow S_n$ transitions, but also by the $S_0 \rightarrow S_1$ transition. The $S_1 \rightarrow S_n$ transition will produce an acoustic grating, and thus an oscillatory signal. Excitation of $S_0 \rightarrow S_1$ with the crossed beams will also produce a grating of electronic excited states. This excited-state grating will decay exponentially at a rate determined by the lifetime. If the probe wavelength is to the red of the $S_0 \rightarrow S_1$ origin and not on an excited-state absorption, the experiment will appear the same as range (1). However, if the probe wavelength falls in the $S_0 \rightarrow S_1$ absorption manifold, or on an excited-state transition, it will be diffracted by the excited-state grating as well as by the acoustic grating.[8] The total signal will appear as an exponential decay with oscillations. Again, the absorption spectrum is directly related to the magnitude of the oscillations. The $S_0 \rightarrow S_1$ transition does not contribute to the oscillations since it deposits negligible heat into the sample immediately upon excitation. The experiments presented below are of this type.

In range (3), the excitation pulses will be absorbed by $S_1 \rightarrow S_n$ transitions, producing heat and an oscillatory signal. There will also be $S_0 \rightarrow S_1$ absorption which will produce both excited S_1 states (excited state grating) and heat. This heat will also contribute to the oscillations. In this case the excited-state spectrum is related to the difference in the amplitude of the oscillations with and without the prepulse. Without the prepulse, the oscillations arise from heating due to the $S_0 \rightarrow S_1^v$ transition, where S_1^v is some vibrational state of S_1. With the prepulse, the oscillations are due to heat from ground-state absorption and excited-state absorption.

Range (3) is always the most difficult spectroscopically. In a conventional optical experiment, it is basically impossible to observe an $S_1 \rightarrow S_n$ transition which is much weaker than an $S_0 \rightarrow S_1^v$ transition at the same wavelength. In this situation, the holographic acoustic method has a considerable advantage. For example, if S_1 is at 18 000 cm^{-1} and S_1^v is at 20 000 cm^{-1}, then an $S_0 \rightarrow S_1^v$ absorption event will deposit only one-tenth the heat of an $S_1 \rightarrow S_n$ transition at 20 000 cm^{-1}. Since the magnitude of the oscillations in the signal depends on the square of the heat deposited (Δn_s^2), the influence of $S_1 \rightarrow S_n$ transition is one hundred times greater than the $S_0 \rightarrow S_1^v$ transition.

The optical discrimination against the ground-state transitions in wavelength range (3) can be quantified in terms of a contrast ratio. From eq 3–6 the ratio of the diffracted signal from excited-state–excited-state transitions to the total signal, ground- and excited-state contributions, is

$$r(\lambda) = \left(\frac{q_1\beta_1}{q_1\beta_1 + q_0\beta_0} \right)^2 \qquad (7)$$

where $q_0\beta_0$ is a measure of the amount of heat rapidly (<100 ps) deposited into the lattice from ground-state absorptions at the grating excitation wavelength λ and $q_1\beta_1$ measures the heat deposited from excited-state–excited-state transitions. Notice that this contrast ratio is wavelength dependent.

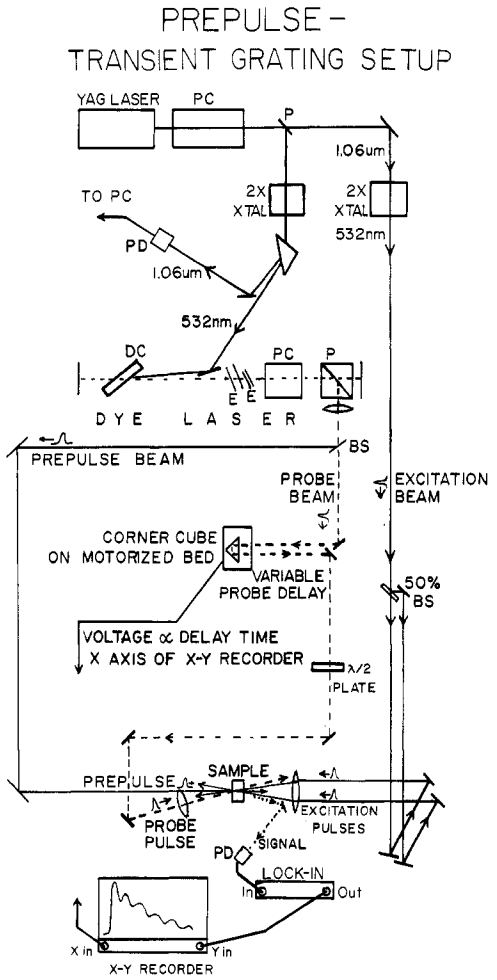

Figure 2. The experimental setup as described in the text: PC, Pockels cell; P, polarizer; PD, photodiode; DC, dye cell; BS, beam splitter; E, etalon.

Experimental Procedures

The details of the laser system and the optical configuration used in these experiments are schematically illustrated in Figure 2. The laser is an optoacoustically Q-switched and mode-locked Nb:YAG system which produces 1.06-μm pulse trains at 400 Hz. Since pulses of 100-ps duration and $\approx$45 μJ in energy are selected by a Pockels cell. The selected single pulse is then frequency doubled to produce a 532-nm, 70-ps, 20-μJ, TEM_{00} pulse. The remaining IR pulse train is also doubled to produce a green pulse train which synchronously pumps a dye laser. The dye laser as configured for these experiments provides 5-μJ, 50-ps pulses in the wavelength range of 550–700 nm. Frequency narrowing of these pulsed to $<\sim 0.2$ cm^{-1} is accomplished by intracavity etalons. A dye laser single pulse is selected by cavity dumping with a Pockels cell.

The green single pulse is passed through a 50% beam splitter, and the resulting two pulses are recombined to form the interference pattern which excites the acoustic waves. The dye laser single pulse is also beam split. One pulse becomes the probe of

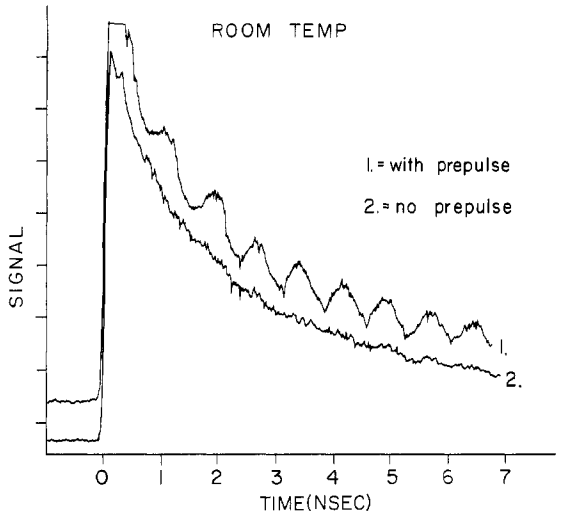

Figure 3. Diffracted signal vs. time for pentacene in *p*-terphenyl host crystals at room temperature. The upper trace, 1, shows diffraction from both an excited-state grating which decays exponentially and an acoustic grating which gives rise to the oscillations. The lower trace, 2, displays only the excited-state grating. Curve 1 is data taken with the excitation prepulse which populates S_1. The acoustic grating occurs because of S_1 to S_n absorption of the crossed 532-nm excitation beams. Curve 2 demonstrates that in the absence of the prepulse, all other conditions identical, the normal grating pulse sequence does not produce an oscillatory signal. The amplitude of the oscillations are proportional to the S_1 to S_n absorption cross section at the grating excitation wavelength.

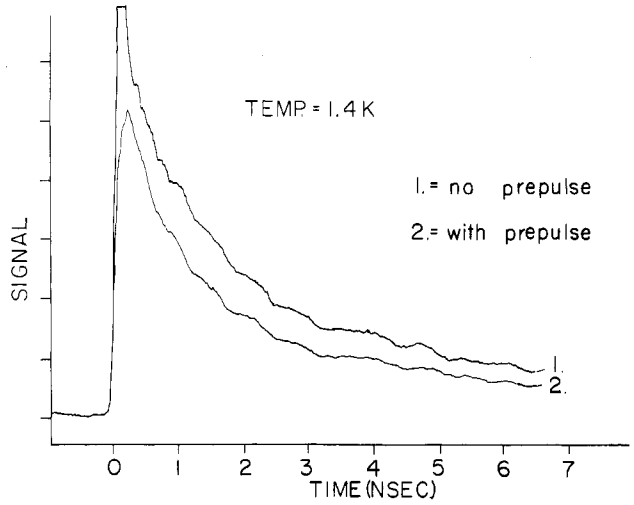

Figure 4. Diffracted signal vs. time for pentacene in *p*-terphenyl at 1.4 K with and without the prepulse. Low amplitude oscillations can be seen in both curves. Trace 2 (with prepulse) is significantly reduced in amplitude because the prepulse produces a substantial number of optical excitations which diminishes the excited-state grating subsequently produced by the excitation pulses. The fact that the magnitude of the oscillations does not change even though the prepulse generates a substantial number of S_1 states demonstrates that there is negligible S_1 to S_n absorption at 532-nm grating excitation wavelength at 1.4 K.

the acoustic response and is brought in at the appropriate angle for Bragg diffraction. The other dye laser pulse becomes the excitation prepulse and it is brought in at normal incidence to the sample, 100 ps before the two green excitation pulses.

Time resolution of the acoustic response is obtained by variably delaying the dye laser probe pulse. A retroreflector is drawn along a precision optical rail by a motor which provides continuous scanning of the probe delay. A ten-turn potentiometer, also driven by the motor, provides a voltage proportional to the probe delay. This voltage drives the *x* axis of an *xy* recorder. The diffracted signal is detected by a large area photodiode and a lock-in amplifier. The output of the lock-in drives the *y* axis of the recorder. When the delay-line motor is scanned, a time-resolved plot of the diffracted signal is obtained.

The system as configured in Figure 2 measures excited-state absorption at the single wavelength (532 nm) of the excitation beams. This is adequate to demonstrate the method and to make an initial investigation of near-resonance contributions to acoustic diffraction. To take excited-state absorption spectra, the single frequency doubled YAG excitation beams would be replaced by tunable dye laser beams. As the wavelength is changed, the size of the acoustic effect is observed.[5] For wide wavelength scans (>100 nm), the angle of the probe beam should be readjusted to obtain maximum diffraction efficiency by maintaining the Bragg angle.

Pentacene in *p*-terphenyl samples were obtained by recrystallizing and extensively zone refining (>200 passes) *p*-terphenyl (Eastman scintillation grade), adding a known amount of pentacene (Aldrich), and growing the crystals under vacuum by the Bridgeman technique. The crystals were cleaved along the $\bar{a}\bar{b}$ plane and orientated by conventional techniques such that the polarizations of the laser pulses were aligned along the *b* axis. A 1-mm-thick single crystal of 1×10^{-4} M/M pentacene was used for the room temperature studies and a 25-μm thick crystal of the same concentration was used for the liquid helium measurements. The low-temperature studies were conducted at 1.4 K by immersing the crystal in pumped liquid helium.

The focusing parameters, used in all the experiments, were an ~200-μm spot size for the grating excitation pulses, ~100-μm spot size for the laser probe, and ~400-μm spot size for the excitation prepulse. The probe was focused by a lens its own focal length away from the sample to ensure a constant spot size as the delay line was scanned. Only diffraction at the Bragg angle was observed. Diffraction efficiencies were on the order of 10^{-3}–10^{-6}.

Results and Discussion

Figure 3 shows time-resolved data from a single crystal of 10^{-4} M/M pentacene in *p*-terphenyl at room temperature with and without the excitation prepulse. The wavelength of the excitation prepulse and the grating probe was tuned to 588 nm, near the peak of the pentacene $S_0 \rightarrow S_1$ absorption band at 591 nm, and doubled YAG (532 nm) was used for the grating excitation pulses. These excitation pulses, which coincide in frequency with a strong ground-state absorption (wavelength range 2), produce long-lived excited states (~10 ns). The periodic change in the ground-state population causes a periodic spatial variation in both the real and imaginary parts of the index of refraction. An excited-state population grating is formed[12] and diffraction is observed from both the excited-state grating and the ultrasonic wave grating.[8] Diffraction from the ultrasonics is observed as modulations superimposed on top of the exponentially decaying excited-state grating.

The data shown without the excitation prepulse (Figure 3, lower curve) decay at a rate proportional to the pentacene lifetime, without modulation. For the power densities used for the grating excitation pulses, very few excited states are created and heat deposition is due to relaxation from the initially excited state at 532 nm to the vibrationally unexcited S_1 level at 588 nm. Diffraction from the excited grating completely masks the diffraction from any ultrasonic wave grating under these conditions. (At higher power densities, strong modulation of the diffracted signal occurs. This power dependence has been previously ascribed to the nonlinear heat deposition arising from consecutive two-photon absorption, $S_0 \rightarrow S_1$ followed by $S_1 \rightarrow S_n$.[8])

The upper curve in Figure 3 shows data taken with the excitation prepulse. All other excitation conditions are identical. The excitation prepulse arrives 100 ps before the grating excitation pulses and selectively populates the pentacene S_1 excited state. The excitation prepulse only depletes about 4% of the ground-state molecules, and the amplitude of the excited-state grating is basically unaffected. Notice, however, that the extent of modulation seen in the upper curve has increased dramatically. The difference in the depth of the modulation with and without the prepulse clearly demonstrates that there is a strong $S_1 \rightarrow S_n$ transition of pentacene at 532 nm. In addition, the relatively small amount of ground-state depletion required to produce significant

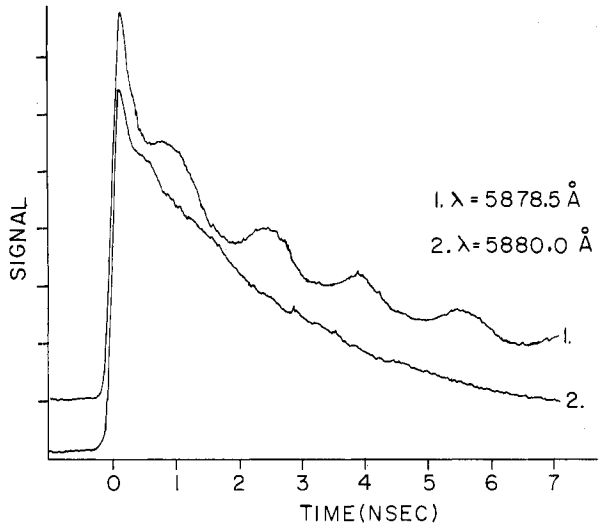

Figure 5. Diffracted signal vs. time for pentacene in *p*-terphenyl at 1.4 K for two probe wavelengths labeled λ in the figure. No prepulse excitation. The data illustrate that substantial acoustic modulation is observed for a probe wavelength near resonance with the strong and narrow pentacene transition at 5880.0 Å. This acoustic diffraction arises because of a density wave induced spectral shift contribution to the diffraction when the probe wavelength is near resonance with a strong and narrow transition.

modulation in the signal demonstrates that the previously observed power dependence for acoustic generation in this system is due to excited-state absorption.

Data taken on the pentacene in *p*-terphenyl system at 1.4 K are in marked contrast to the room temperature data. At low temperature, pentacene substitutes into the *p*-terphenyl lattice in four nonequivalent sites producing four narrow ($\sim$3 cm^{-1}) very strong absorption origins.[15] The O_3 origin at 17 006 cm^{-1} was examined since it is the most spectrally isolated of the four peaks. The data are shown in Figure 4. The upper curve is without the prepulse, and the lower curve are data observed with the prepulse. Excitation conditions are the same as those used for the room temperature data. The probe and prepulse wavelength are nearly resonant with the 17 006-cm^{-1} transition. In the room temperature data (Figure 3) the overall signal strengths with and without prepulse are basically identical (note baseline displacement). However, the 1.4 K signal (Figure 4) with the prepulse is significantly reduced in intensity relative to the signal without the prepulse (note the baselines coincide). The decrease in the overall diffracted probe pulse signal with the prepulse demonstrates that the prepulse has significantly depleted the ground-state population, thereby reducing the amplitude of the excited-state grating. Notice, however, that despite the large number of excited states populated by the excitation prepulse, there is no increase in the depth of modulation of the signal. The lack of prepulse effect demonstrates that the S_1 to S_n absorption cross section at 532 nm is negligible at 1.4 K. There is no significant contribution to the ultrasonic amplitude from excited-state absorption. The lack of excited-state–excited-state absorption at 532 nm is presumably due to the substantial narrowing of the spectral lines at low temperature, resulting in 532 nm not being on resonance with an $S_1 \rightarrow S_n$ transition at 1.4 K.

Recently, it has been predicted that in addition to the normal bulk number density phase gratings, ultrasonic diffraction can arise from ultrasonic induced changes in the frequency of an electronic transition which is near resonant with the probe wavelength.[8] Extrapolations from static density studies of spectral shifts[8,16] have indicated that the density oscillations produced by ultrasonic waves should be capable of modulating the spectral position of an absorption band by $\sim$0.1–0.01 cm^{-1}. The exact magnitude of the shift depends on the amplitude of the ultrasonic wave and the strength of the coupling between the electronic energy levels and the acoustic phonon. An ultrasonic induced spectral shift imposes sinusoidal variations in the optical density of the sample and leads to enhanced diffraction for probe wavelengths near the band origin. For optical line widths on the order of 1 cm^{-1}, a 0.1–0.01-cm^{-1} change in the position of the line maximum would constitute a large change in the optical properties of the sample. Ultrasonic diffraction in this case should be completely dominated by spectral shift effects.[8] Pentacene in *p*-terphenyl at liquid helium temperatures provides an excellent system to investigate this mechanism of ultrasonic diffraction.

Additional grating diffraction data for pentacene in *p*-terphenyl at 1.4 K (no excitation prepulse) are shown in Figure 5. Data for two different probe wavelengths are depicted, one on resonance with the line center, and the other $\sim$4-cm^{-1} blue of the maximum. The probe wavelength dependence of the modulation depth has been discussed in detail previously.[8] (Note the extent of modulation in the 5878.5-Å data is greater than in Figure 4 because the probe wavelength is further off resonance.) The important observation from this data is that the amplitude of the ultrasonic grating is on the order of the excited-state grating for probe wavelengths near the band origin. When the temperature was lowered from room temperature to 1.4 K, the diffraction efficiency of the excited-state grating increased by approximately a factor of 100. This increase is from the decrease in the line width and the corresponding increase in the absorption strength of the transition.

At low temperatures, the heat capacity decreases dramatically, but in general the thermoelastic constants of crystals decrease in a similar manner. The net result is that for the same amount of energy converted to heat at room temperature and at 1.4 K, the induced ultrasonic waves should have about the same amplitude. If the amplitudes of the strain waves are similar at the two temperatures, in the low-temperature sample the excited-state grating should completely overwhelm any contribution to the signal from the acoustic bulk number density phase grating.

There are two possible reasons why the acoustic grating manifests itself in the low-temperature sample. The first is that the acoustic amplitude is much greater at low temperature because a strong $S_1 \rightarrow S_n$ excited-state transition deposits great quantities of energy into the sample as heat. *The prepulse coherent photoacoustic experiments conclusively rule out this possibility.*

The other possibility is that the strain wave is approximately the same size, but the coupling between the acoustic grating and the probe radiation field is greater, i.e., there are additional contributions to the diffraction efficiency in the low-temperature system. As discussed above, these additional contributions are predicted to arise from density wave induced spectral shifts.[8] The spectral shifts produce both phase and amplitude gratings. For intense narrow lines which are probed near resonance, the spectral shift grating diffraction can far outweigh the bulk number density phase grating diffraction.[8] Bulk number density phase grating diffraction is responsible for all previous observations of diffraction from acoustic gratings and for all optoacoustic devices. The results presented here demonstrate that greatly increased acoustic diffraction efficiency can be obtained by using a probe wavelength near a very intense and narrow transition. The experiments suggest that the increased efficiency arises from additional spectral shift contributions to diffraction. A detailed comparison between the probe wavelength dependence of the diffraction efficiency for probe wavelengths near resonance and theoretical predictions based on the spectral shift model[8] are necessary to confirm the spectral shift mechanism.

Acknowledgment. M.P. acknowledges a USA–France exchange postdoctoral fellowship. This work was supported by the National Science Foundation, Division of Material Research (Grant DMR 79-20380). M.D.F. acknowledges the Simon Guggenheim Memorial Foundation for Fellowship support that contributed to this research.

Registry No. Pentacene, 135-48-8; *p*-terphenyl, 92-94-4.

(15) R. W. Olson and M. D. Fayer, *J. Phys. Chem.*, **84**, 2001 (1980).
(16) P. F. Jones, *J. Chem. Phys.*, **48**, 5448 (1968); B. Y. Okamoto and H. G. Drickamer, *ibid.*, **61**, 2870 (1974); J. Donnini, **71**, 1543 (1974).